nature immunology

Interactions between PD-1 and PD-L1 promote tolerance by blocking the TCR–induced stop signal

Brian T Fife[1,2], Kristen E Pauken[2], Todd N Eagar[1,3], Takashi Obu[2], Jenny Wu[1], Qizhi Tang[1,4], Miyuki Azuma[5], Matthew F Krummel[6] & Jeffrey A Bluestone[1]

Programmed death 1 (PD-1) is an inhibitory molecule expressed on activated T cells; however, the biological context in which PD-1 controls T cell tolerance remains unclear. Using two-photon laser-scanning microscopy, we show here that unlike naive or activated islet antigen–specific T cells, tolerized islet antigen–specific T cells moved freely and did not swarm around antigen-bearing dendritic cells (DCs) in pancreatic lymph nodes. Inhibition of T cell antigen receptor (TCR)-driven stop signals depended on continued interactions between PD-1 and its ligand, PD-L1, as antibody blockade of PD-1 or PD-L1 resulted in lower T cell motility, enhanced T cell–DC contacts and caused autoimmune diabetes. Blockade of the immunomodulatory receptor CTLA-4 did not alter T cell motility or abrogate tolerance. Thus, PD-1–PD-L1 interactions maintain peripheral tolerance by mechanisms fundamentally distinct from those of CTLA-4.

Autoimmunity results from the breakdown of processes designed to maintain self-tolerance. The growing list of costimulatory and inhibitory receptors that influence immune cell activation has been a central concern in immunology for over two decades. CTLA-4 (CD152) is a well established negative regulator of T cell function[1]. CTLA-4 is rapidly expressed on the surface of T cells after activation and is highly upregulated by engagement of the costimulatory molecule CD28 (ref. 1). CTLA-4 ligation antagonizes early T cell activation by inhibiting interleukin 2 (IL-2) production, cell cycle progression and T cell antigen receptor (TCR) signaling[2,3]. CTLA-4 and CD28 share the ligands B7-1 (CD80) and B7-2 (CD86)[4]. Mice deficient in CTLA-4 develop lymphoproliferative disease and die within 3–4 weeks of birth[5], which adds further evidence of the critical role of CTLA-4 in controlling T cell responses and immune homeostasis.

Programmed death 1 (PD-1 (CD279)) is an inhibitory molecule found on the surface of activated B cells and T cells that has been linked to immune tolerance[6]. PD-1 is a member of the CD28 and CTLA-4 immunoglobulin superfamily and interacts with two B7 family ligands, PD-L1 (CD274) and PD-L2 (CD273)[4]. PD-L1 is widely distributed on leukocytes and nonhematopoietic cells in lymphoid and nonlymphoid tissues, including pancreatic islets, whereas PD-L2 is expressed exclusively on dendritic cells (DCs) and monocytes[7,8]. The PD-1 signaling pathway limits viral clearance during chronic infection by creating an unresponsive state in virus-specific $CD8^+$ T cells called 'exhaustion'[9]. In an autoimmune setting, PD-1 is essential for maintaining T cell anergy and preventing autoimmunity[10,11]. Genetic deletion of PD-1 results in profound and complex multiorgan autoimmune destruction[4]. Similarly, blocking PD-1–PD-L1 interactions accelerates spontaneous autoimmune diabetes[12] and reverses immune tolerance[10,11]. Together these data support the idea that PD-1 serves a central role as a major inhibitory pathway controlling immunity and suggest that exhaustion and peripheral tolerance are linked mechanistically.

Several theories have emerged to explain the mechanism by which PD-1 suppresses T cell activation. PD-L1 may act passively by competing directly with CD28 for B7-1 binding[13]. In addition, PD-1 may directly recruit phosphatases such as SHP-1 and SHP-2, which interfere with TCR signaling[4,14–16]. However, the effects of PD-1 engagement during T cell activation are unclear, as *in vitro* models have not adequately demonstrated the inhibitory activity of PD-1 (ref. 17). *In vivo* studies of PD-1-mediated inhibition have been limited to global effects on immunity with little evidence that PD-1 engagement directly controls T cell signaling.

A well-defined, antigen-specific tolerance model has been used to examine the cellular basis of immunological tolerance with antigen-pulsed and fixed antigen-presenting cells (APCs)[10]. Administration of the islet antigen peptide mimic p31 coupled to chemically fixed APCs reversed diabetes and induced robust, long-term inactivation of islet-specific BDC2.5 TCR–transgenic T cells. Tolerized T cells did not proliferate or produce cytokines in response to TCR stimulation. Although both PD-1 and CTLA-4 interactions were critical for the induction of tolerance, long-term maintenance of the anergic state depended on PD-1–PD-L1 interactions but not on CTLA-4 interactions in the inflamed tissue[10]. These results indicate that a cell-intrinsic mechanism maintains tolerance in the setting of continual exposure to autoantigen.

[1]UCSF Diabetes Center, Department of Medicine, University of California, San Francisco, California, USA. [2]Department of Medicine, Center for Immunology, University of Minnesota, Minneapolis, Minnesota, USA. [3]Department of Neurology, University of Texas Southwestern, Dallas, Texas, USA. [4]Department of Surgery, University of California, San Francisco, California, USA. [5]Department of Molecular Immunology, Tokyo Medical and Dental University, Tokyo, Japan. [6]Department of Pathology, University of California, San Francisco, California, USA. Correspondence should be addressed to B.T.F. (bfife@umn.edu).

Received 12 June; accepted 12 August; published online 27 September 2009; doi:10.1038/ni.1790

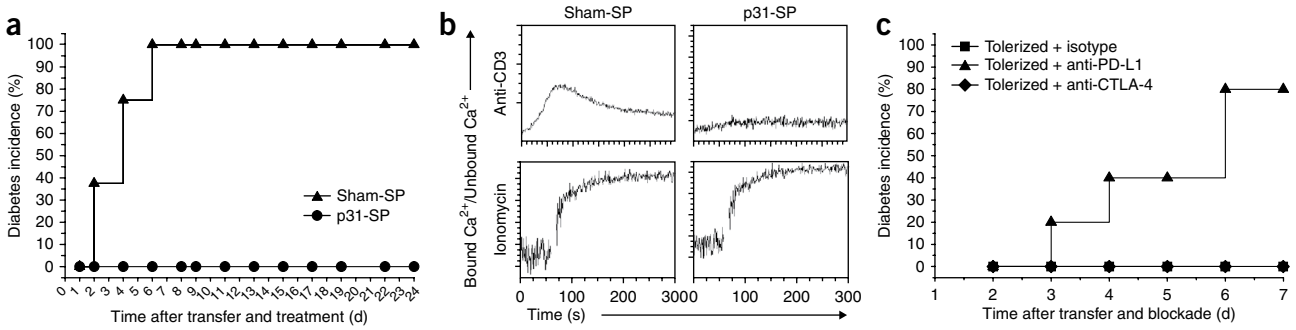

Figure 1 Antigen-specific tolerance blocks diabetes, TCR signaling and Ca^{2+} flux in a PD-L1-dependent manner. (**a**) Diabetes incidence in NOD mice given activated BDC2.5 T cells, followed by treatment with p31-SP ($n = 8$ mice; p31-tolerized) or sham-SP ($n = 8$ mice; activated control) on the same day. (**b**) Ca^{2+} flux in BDC2.5 TCR–transgenic $CD4^+$ T cells obtained from mice treated *in vivo* with p31-SP or sham-SP, then purified, loaded with the calcium indicator Indo-1 and activated with anti-CD3 (5 μg/ml) and crosslinking antibody or ionomycin. (**c**) Development of type 1 diabetes in naive recipient mice given 2×10^6 p31-SP-tolerized BDC2.5 TCR–transgenic T cells, followed by anti-PD-L1, anti-CTLA-4 or isotype-matched control antibody ($n = 5$ mice per group), monitored by measurement of blood glucose. Data are representative of three or more independent experiments (**a**,**b**) or are from two independent experiments (**c**).

Imaging advances have allowed the use of multiphoton laser-scanning microscopy (MPLSM) to visualize T cells in lymph nodes and nonlymphoid tissues *in vivo* at the single-cell level[18]. Several groups have described the highly dynamic movement of $CD4^+$ and $CD8^+$ T cells as well as DCs during T cell priming and tolerance induction[19–23]. Naive circulating T cells enter the lymph node through high endothelial venules and move on a network of stromal cells called 'fibroblastic reticular cells', which define the potential location and migratory range of T cells[24]. The fibroblastic reticular cells also provide a substrate for resident DCs to sample and display antigen to passing T cells. As T cells migrate along the fibroblastic reticular cell 'highway', they probe DCs for signals and antigen[24]. Initial interactions may be transient, but antigen recognition results in T cell swarming, the formation of stable T cell–DC conjugates and T cell arrest[25,26]. TCR ligation results in 'stop signals' that decrease T cell motility and are required for stable T cell–DC conjugate formation and development of the immunological synapse[21,26]. Prolonged T cell–DC interactions are critical for full T cell activation, proliferation and cytokine production[27–29]. However, dynamic T cell movement during the long-term maintenance of tolerance has not been well described.

Here we examined the biological roles of the PD-1 and CTLA-4 inhibitory pathways during autoimmunity using multiphoton imaging techniques. PD-1 suppressed TCR-driven stop signals in the pancreatic islets, and blockade of PD-1 or PD-L1 inhibited T cell migration, prolonged T cell–DC engagement, enhanced T cell cytokine production, boosted TCR signaling and abrogated peripheral tolerance. CTLA-4 blockade left T cell motility and tolerance unaltered. Thus, our findings suggest that PD-1 and CTLA-4 have fundamentally distinct roles in the maintenance of peripheral tolerance and autoimmunity.

RESULTS

PD-1-dependent, islet antigen–specific tolerance

Insulin-coupled, ethylene carbodiimide–fixed APCs have a profound effect on the development of spontaneous type 1 diabetes in the nonobese diabetic (NOD) mouse[10]. A single injection of antigen-pulsed, fixed splenocytes prevents and even reverses type 1 diabetes after disease onset. A critical role for PD-1 but not CTLA-4 has been identified in the maintenance of tolerance induced by injection of insulin-coupled, fixed splenocytes[10]. Here we adapted that model using islet antigen–specific BDC2.5 TCR–transgenic T cells to define the role of PD-1 and CTLA-4 in the maintenance of peripheral tolerance.

We tracked the movement of fluorochrome-labeled diabetogenic BDC2.5 $CD4^+$ T cells *in vivo* by MPLSM. We induced type 1 diabetes by adoptive transfer of activated BDC2.5 T cells into naive prediabetic NOD recipient mice. Control recipient mice injected with splenocytes coupled with an irrelevant antigen (sham-SP) developed severe type 1 diabetes within 6 d of T cell transfer (**Fig. 1a**). Injection of splenocytes coupled to the peptide p31 (p31-SP), an islet antigen mimetope recognized by the BDC2.5 TCR[30], prevented autoimmune diabetes and resulted in lower T cell proliferation and cytokine production (**Fig. 1a** and data not shown). To test if T cell unresponsiveness was consistent with T cell anergy, we measured Ca^{2+} flux 1 week after tolerance induction by p31-SP. Published work has demonstrated that TCR-induced Ca^{2+} signals are associated with T cell motility and stable interactions with APCs[25]. BDC2.5 T cells isolated from mice tolerized with p31-SP did not flux Ca^{2+} in response to strong secondary TCR stimulation with antibody to CD3 (anti-CD3), but cells from mice injected with sham-SP had normal Ca^{2+} responses (**Fig. 1b**). Furthermore, phosphorylation of the TCR ζ-chain and the mitogen-activated protein kinase Erk was lower in T cells isolated from mice treated with p31-SP than in those treated with sham-SP (data now shown). These data provide evidence that exposure to p31-SP *in vivo* resulted in a TCR-proximal signaling defect.

Next we investigated the role of PD-1 and CTLA-4 in the maintenance of this unresponsive state. We transferred T cells from p31-SP-tolerized, BDC2.5 TCR–transgenic mice into naive recipients, then injected the recipients with anti-PD-L1, anti-CTLA-4 or isotype-matched control antibody. Blocking PD-L1 led to the reversal of tolerance and rapid precipitation of clinical diabetes (**Fig. 1c**). In contrast, CTLA-4 blockade did not affect clinical disease (**Fig. 1c**). Anti-PD-L1 also led to more accumulation of antigen-specific BDC2.5 T cells in the pancreatic lymph nodes (PLNs), but anti-CTLA-4 did not (data not shown). Together these results demonstrate that antigen-specific tolerance regulates autoimmune diabetes and that PD-L1, but not CTLA-4, has a critical role in the maintenance of this anergic state.

PD-1 but not CTLA-4 prevents T cell stop signals

To ascertain the roles of PD-1 and CTLA-4 during the maintenance of tolerance, we developed a system to study the dynamic movement of tolerized T cells in intact mouse lymph nodes by MPLSM. As tolerance induced by p31-SP correlated with impaired calcium signaling, and PD-1 but not CTLA-4 maintained this

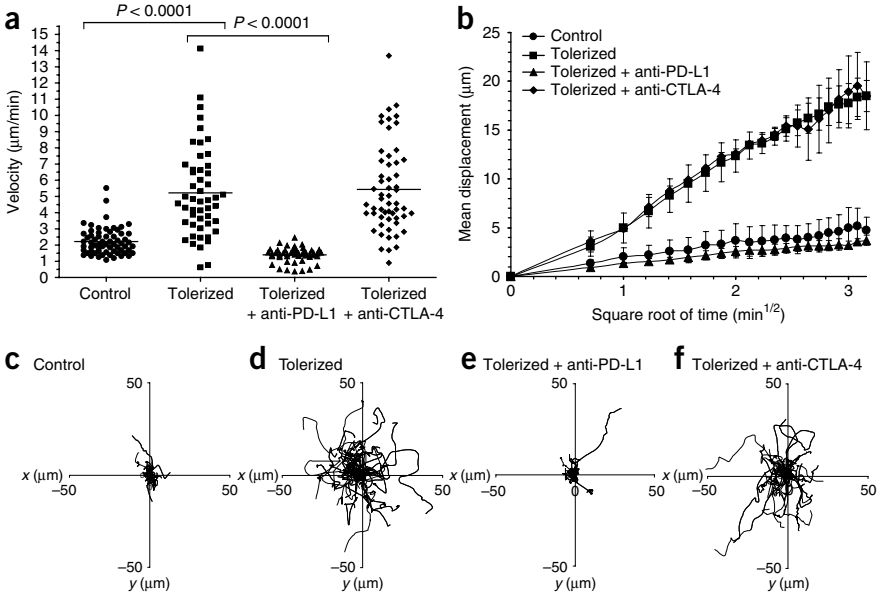

Figure 2 PD-1–PD-L1 but not CTLA-4 prevents the T cell stop signal. Multiphoton image analysis of the dynamic migration of CMTMR-labeled control or tolerized BDC2.5 CD4$^+$ T cells adoptively transferred into NOD.CD11c-YFP recipient mice and visualized in islet antigen–containing PLNs. (**a**) Velocity of BDC2.5 CD4$^+$ T cells that were activated *in vitro* and transferred into CD11c-YFP recipient mice (Control) or were activated *in vitro*, tolerized *in vivo* with p31-SP, transferred into recipient mice that were subsequently injected with isotype-matched control antibody (Tolerized), anti-PD-L1 (Tolerized + anti-PD-L1) or anti-CTLA-4 (Tolerized +anti-CTLA-4). Each symbol represents an individual cell; small horizontal lines indicate mean velocity. *P* values, unpaired Student's *t*-test. (**b**) Displacement of T cells in PLNs of mice that received control T cells or tolerized T cells plus isotype-matched control antibody, anti-PD-L1 or anti-CTLA-4, plotted against the square root of time (mean ± s.d. of multiple imaging data sets). Time-lapse recordings corresponding to this region for each group are in **Supplementary Movies 1–4**. (**c–f**) Superimposed 10-minute tracks in the *xy* plane of 40–60 randomly selected T cells from each treatment group in **a**,**b**, with starting coordinates set from the origin (0.0). Each line represents the path of one cell. Data are representative of three or more independent experiments.

tolerant state, we tested the hypothesis that PD-L1 prevents the TCR-mediated T cell stop signal associated with T cell activation and type 1 diabetes. Antigen-specific T cells swarm and cluster when they enter antigen-containing PLNs[31]. Thus, we compared the migratory activity of activated control BDC2.5 T cells with that of tolerized BDC2.5 T cells. We isolated BDC2.5 Thy-1.1$^+$ CD4$^+$ T cells from mice treated with sham-SP or p31-SP, labeled the cells with cell-tracking dye CMTMR and transferred them into NOD mice expressing a transgene encoding yellow fluorescent protein (YFP) driven by the promoter of the gene encoding CD11c. This CD11c-YFP mouse allows tracking of the *in vivo* movements of CD11c$^+$ DCs[32]. We compared the velocity and displacement of control and tolerized T cells in islet antigen–bearing PLNs 18–24 h after T cell transfer. Control activated BDC2.5 T cells slowed down and swarmed in antigen-bearing PLNs, with a velocity of 2.2 ± 0.1 μm/min (**Fig. 2a** and **Supplementary Movie 1**), similar to results reported before[31]. In contrast, the tolerized T cells did not swarm in antigen-containing PLNs and had a mean velocity of 5.2 ± 0.4 μm/min (**Fig. 2a** and **Supplementary Movie 2**), similar to results reported for lymph nodes not bearing antigen[31].

Next we designed experiments to assess the effect of PD-1 and CTLA-4 on T cell motility during the maintenance phase of tolerance. As PD-L1, but not PD-L2, is required for the maintenance of tolerance, we examined the effect of PD-L1-blocking antibodies[10]. After PD-L1 blockade, the tolerized T cells slowed and swarmed with a velocity of 1.4 ± 0.1 μm/min, in contrast to the velocity of 5.2 μm/min observed after treatment with isotype-matched control antibody ($P < 0.0001$; **Fig. 2a** and **Supplementary Movie 3**). PD-1 blockade produced similar effects on T cell swarming and stop signals (data not shown). Together these data support the idea that PD-1–PD-L1 interactions are needed to mediate tolerance and prevent T cell stop signals.

CTLA-4 blockade, in contrast, did not affect the movement of tolerized T cells, as tolerized T cells maintained a mean velocity of 5.4 ± 0.4 μm/min after CTLA-4 blockade (**Fig. 2a** and **Supplementary Movie 4**). We next assessed T cell motility by measuring the displacement of T cells plotted against the square root of time (motility coefficient (*M*)). This measurement reflects not simply the total distance traveled but instead displacement from the point of origin. Consistent with published reports[22,33,34], antigen encounter resulted in little displacement of control T cells ($M = 0.32 \pm 0.16$ μm^2/min; **Fig. 2b**). In contrast, the displacement of tolerized BDC2.5 T cells was significantly greater ($M = 6.65 \pm 0.21$ μm^2/min ($P < 0.0001$); **Fig. 2b**), indicative of a process in which activated antigen-specific T cells stop and are engaged in stable interactions with APCs while the tolerized T cells move freely in the PLNs. As suggested by the change in velocity, blockade of PD-1–PD-L1 interactions resulted in less displacement and arrest of tolerized T cells ($M = 0.19 \pm 0.06$ μm^2/min; **Fig. 2b**). CTLA-4 blockade, in contrast, did not result in less T cell displacement ($M = 7.0 \pm 4.6$ μm^2/min; **Fig. 2b**). By tracking individual cells and plotting the superimposed tracks from the origin for each group, we were able to demonstrate the limited movement of activated cells compared with that of tolerized T cells (**Fig. 2c**,**d**). PD-L1 blockade induced T cell arrest and limited displacement (**Fig. 2e**), similar to that of activated T cells (**Fig. 2c**), but dissimilar from the effects of CTLA-4 blockade (**Fig. 2f**). These results demonstrate a fundamental distinction between the functions of PD-1 and CTLA-4 and suggest that PD-L1 blockade enhances T cell stop signals.

To investigate if PD-1–PD-L1 interactions function in an antigen-dependent or antigen-independent manner, we investigated the migratory activity of BDC2.5 T cells in antigen-deficient inguinal lymph nodes (ILNs). We compared the velocity and displacement of control and tolerized T cells 18–24 h after T cell transfer. In all cases, T cells migrated freely in the ILNs with similar velocities, displacement and motility, and migration was independent of T cell activation or tolerance and the presence or absence of PD-L1 or CTLA-4 blockade (**Fig. 3** and **Supplementary Movies 5–8**). Thus, the enhanced stop signal and confined displacement required TCR engagement with islet antigen(s) (PLNs versus ILNs) as well as the disruption of PD-L1 ligation. It is notable that administration of anti-PD-L1 did not affect the movement of naive, nontolerized polyclonal T cells (**Supplementary Movie 9**). This was probably due to the fact that tolerized T cells have high surface expression of PD-1, whereas naive

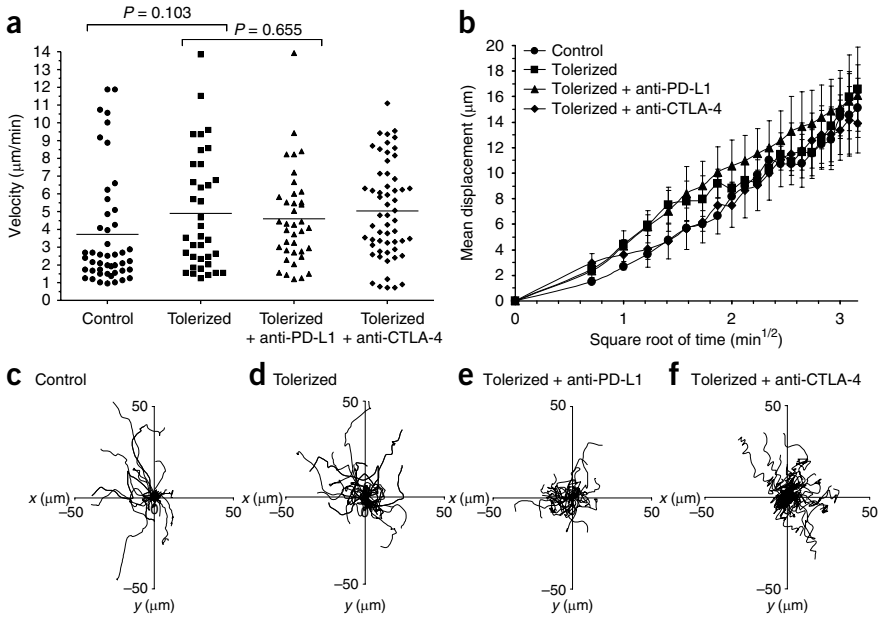

Figure 3 PD-L1 inhibition requires antigen. Multiphoton image analysis of the dynamic migration of CMTMR-labeled control or tolerized diabetogenic BDC2.5 CD4$^+$ T cells adoptively transferred into NOD.CD11c-YFP recipient mice and visualized in ILNs not containing islet antigen. (**a**) Velocity of BDC2.5 CD4$^+$ T cells that were activated *in vitro* and transferred into CD11c-YFP recipient mice or activated *in vitro*, tolerized with p31-SP *in vivo*, transferred to recipient mice that were subsequently injected with isotype-matched control antibody, anti-PD-L1 or anti-CTLA-4. Each symbol represents an individual cell; small horizontal lines indicate mean velocity. *P* values, unpaired Student's *t*-test. (**b**) Displacement of T cells in ILNs of mice that received control T cells or tolerized T cells plus isotype-matched control antibody, anti-PD-L1 or anti-CTLA-4, plotted against the square root of time (mean ± s.d. of multiple imaging data sets). Time-lapse recordings corresponding to this region for each group are in **Supplementary Movies 5–8**. (**c–f**) Superimposed 10-minute tracks in the *xy* plane of 40–50 randomly selected T cells from each treatment group in **a**,**b**, with starting coordinates set from the origin (0.0). Each line represents the path of one cell. Data are representative of three or more independent experiments.

T cells do not[10,35]. These results reinforce the idea that antigen is required for the stop signal and that PD-1 normally functions to inhibit T cell activation by preventing T cell arrest.

PD-1 inhibits T cell movement in the islets

PD-1-mediated control of immune responses depends on interactions between PD-1 on T cells and PD-L1 in tissues[10,11]. Thus, we sought to determine if the effects of PD-1–PD-L1 blockade had similar effects in the autoimmune target tissue, the pancreatic islets, as was the case in antigen-draining PLNs. To accomplish this, we developed a system to analyze T cell motility *in vivo* in pancreatic islets of Langerhans by MPLSM. We transferred islets from NOD.MIP-eGFP mice under the kidney capsule of recipient NOD.SCID mice. The transgenic NOD.MIP-eGFP mice express enhanced green fluorescent protein (eGFP) under the control of the promoter of the mouse gene encoding insulin 1. One week after islet transplantation, the NOD.SCID recipient mice received CMTMR-labeled tolerized BDC2.5 Thy-1.1$^+$ T cells. After T cell transfer, we gave recipient mice anti-PD-L1, anti-CTLA-4 or isotype-matched control antibody and tracked cell movement. As in the antigen-containing PLNs, tolerized BDC2.5 T cells moved rapidly in the islet transplants in mice treated with isotype-matched control antibody (velocity = 6.2 ± 0.3 μm/min; **Fig. 4a** and **Supplementary Movie 10**). PD-L1 blockade resulted in lower velocity (3.3 ± 0.2 μm/min; **Fig. 4a** and **Supplementary Movie 11**), whereas CTLA-4 blockade did not affect the migration of previously tolerized T cells despite the presence of antigen (velocity = 6.6 ± 0.3 μm/min; **Fig. 4a** and

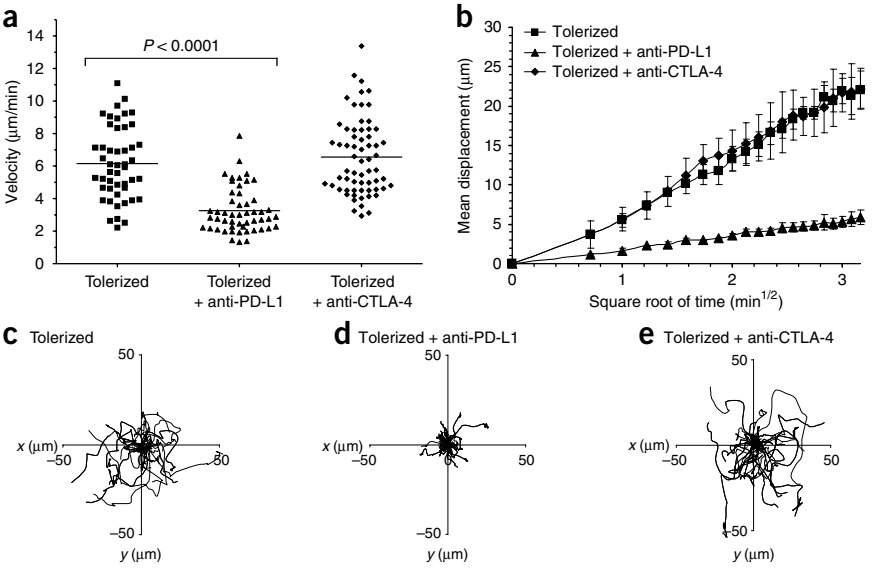

Figure 4 PD-L1 inhibits T cell movement in the islets. Multiphoton microscopy of the dynamics and motility of CMTMR-labeled tolerized BDC2.5 CD4$^+$ T cells (red) visualized in NOD.SCID mice previously transplanted with MIP.eGFP islets (green) under the kidney capsule. (**a**) Velocity of BDC2.5 CD4$^+$ T cells tolerized *in vivo* with p31-SP and transferred into NOD.SCID recipient mice that were subsequently injected with isotype-matched control antibody (Tolerized), anti-PD-L1 (Tolerized +anti-PD-L1), or anti-CTLA-4 (Tolerized +anti-CTLA-4). Each symbol represents an individual cell; small horizontal lines indicate mean velocity. *P* value, unpaired Student's *t*-test. Time-lapse recordings corresponding to this region for each treatment group are in **Supplementary Movies 10–12**. (**b**) Displacement of T cells in islets of mice that received tolerized T cells plus isotype-matched control antibody, anti-PD-L1 or anti-CTLA-4, plotted against the square root of time (mean ± s.d. of multiple imaging data sets). (**c–e**) Superimposed 10-minute tracks in the *xy* plane of 43–60 randomly selected T cells from each treatment group in **a**,**b**, with starting coordinates set from the origin (0.0). Each line represents the path of one cell. Data are representative of at least three independent experiments.

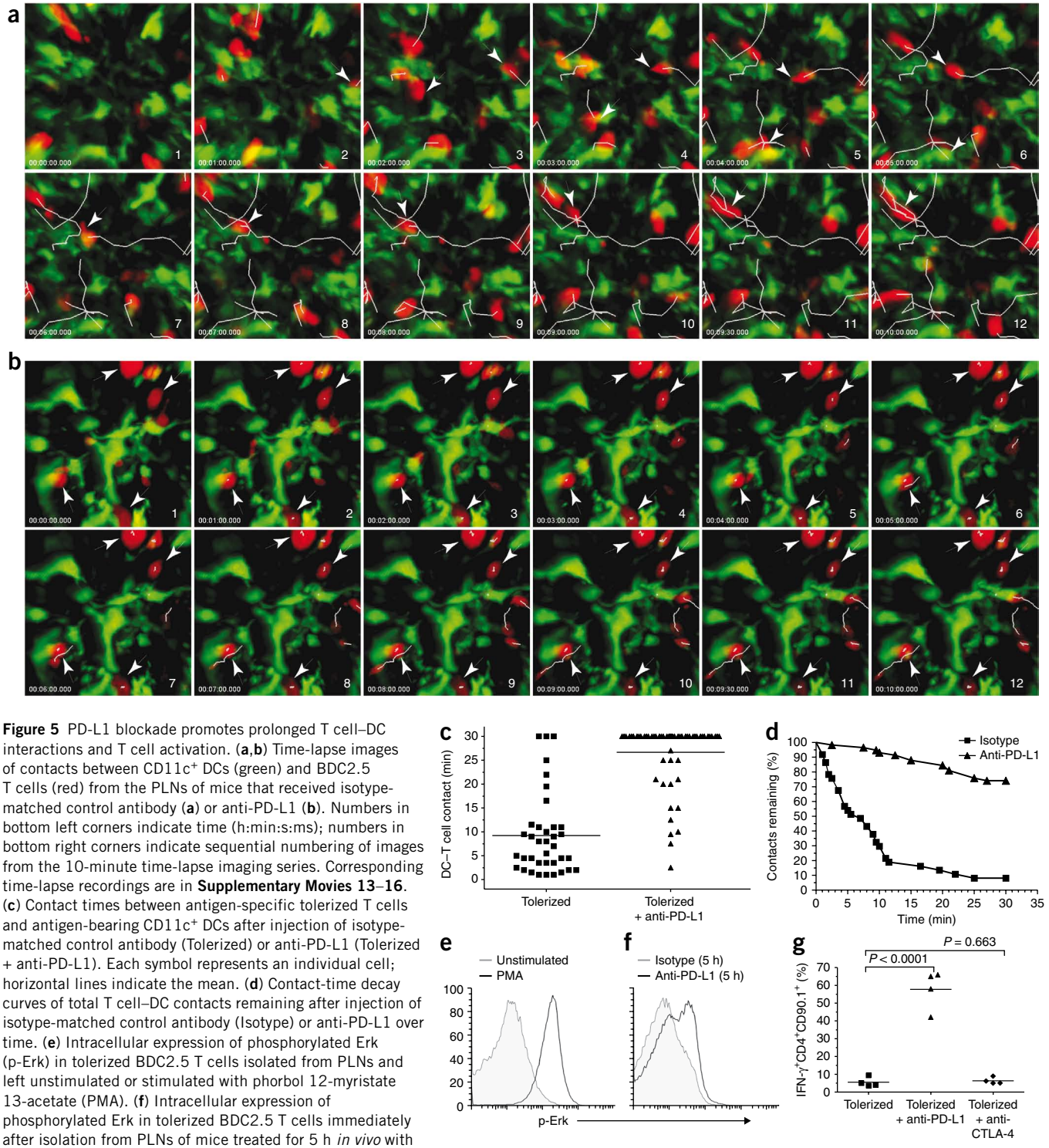

Figure 5 PD-L1 blockade promotes prolonged T cell–DC interactions and T cell activation. (**a**,**b**) Time-lapse images of contacts between CD11c$^+$ DCs (green) and BDC2.5 T cells (red) from the PLNs of mice that received isotype-matched control antibody (**a**) or anti-PD-L1 (**b**). Numbers in bottom left corners indicate time (h:min:s:ms); numbers in bottom right corners indicate sequential numbering of images from the 10-minute time-lapse imaging series. Corresponding time-lapse recordings are in **Supplementary Movies 13–16**. (**c**) Contact times between antigen-specific tolerized T cells and antigen-bearing CD11c$^+$ DCs after injection of isotype-matched control antibody (Tolerized) or anti-PD-L1 (Tolerized + anti-PD-L1). Each symbol represents an individual cell; horizontal lines indicate the mean. (**d**) Contact-time decay curves of total T cell–DC contacts remaining after injection of isotype-matched control antibody (Isotype) or anti-PD-L1 over time. (**e**) Intracellular expression of phosphorylated Erk (p-Erk) in tolerized BDC2.5 T cells isolated from PLNs and left unstimulated or stimulated with phorbol 12-myristate 13-acetate (PMA). (**f**) Intracellular expression of phosphorylated Erk in tolerized BDC2.5 T cells immediately after isolation from PLNs of mice treated for 5 h *in vivo* with isotype-matched control antibody or anti-PD-L1. (**g**) Flow cytometry of pancreas-infiltrating CD4$^+$IFN-γ$^+$ (YFP$^+$) cells from BDC2.5 Thy-1.1$^+$ Yeti mice tolerized *in vivo* with p31-SP, followed by treatment with anti-PD-L1, anti-CTLA-4 or isotype-matched control antibody and analysis 3 d later. *P* values, unpaired Student's *t*-test. Data are representative from at least three independent experiments (**a**–**e**,**g**) or are from two independent experiments (**f**).

Supplementary Movie 12). We also measured the displacement of previously tolerized T cells in the islet transplants. We observed free and apparently unconstrained migration of tolerized T cells in recipient mice treated with isotype-matched control antibody or anti-CTLA-4 (isotype control, $M = 15.8 \pm 5.3$ μm^2/min; CTLA-4, $M = 10.1 \pm 2.3$ μm^2/min). The slope of these two curves was a straight line representing free and random walking in the target tissue and did not correspond to directed migration[33]. PD-L1 blockade, however, attenuated T cell motility and resulted in less T cell displacement than that in mice treated with isotype-matched control antibody ($M = 0.5 \pm 0.3$ μm^2/min; **Fig. 4b**). Tracking of individual cells confirmed those results (**Fig. 4c–e**). These data show that

PD-1–PD-L1 interactions modulate TCR-induced swarming and arrest activities in autoimmune target tissues.

PD-L1 blockade enhances stable T cell–DC interactions

The studies described above suggest that blocking PD-1–PD-L1 interactions leads to less T cell movement and thus may provide the opportunity for extended interactions between antigen-specific T cells and antigen-bearing APCs. Prolonged interactions between T cells and DCs is critical for full T cell activation[27,29]. We hypothesized that PD-1 normally functions to prevent the stable T cell–DC contacts that are required for full T cell activation. To test our idea, we used the adoptive transfer and imaging system described above to measure the dwell time of antigen-specific T cells with DCs. We labeled BDC2.5 T cells red with CMTMR and transferred them into NOD.CD11c-YFP recipient mice and then determined T cell–DC interaction times in antigen-containing sites (PLNs) and antigen-deficient sites (ILNs). Tolerized T cells did not slow down or form stable contacts with tissue DCs (**Fig. 5a** and **Supplementary Movie 13**). In contrast, many stable conjugates formed between T cells and $CD11c^+$ DCs after PD-L1 blockade (**Fig. 5b** and **Supplementary Movie 14**). PD-L1 blockade was associated with greater duration of T cell–DC contacts (**Fig. 5c**). Notably, most T cells from mice treated with anti-PD-L1 interacted with tissue-specific DCs for the entire duration of the imaging experiment (30 min), with a mean dwell time of 26.6 ± 6.8 min, compared with 9.2 ± 8.5 min for tolerized T cells from mice treated with isotype-matched control antibody ($P < 0.0001$; **Fig. 5c**). In addition, approximately 75% of labeled tolerized T cells that made contact with DCs maintained these contacts for the entire imaging sequence of 30 min in anti-PD-L1-treated mice, whereas only 8% of tolerized T cells maintained DC interactions in mice treated with isotype-matched control antibody (**Fig. 5d** and **Supplementary Movies 15** and **16**). Stable conjugates in the ILNs were not readily detectable in either group (data not shown), consistent with the idea that antigen is required for these interactions. Together these data suggest that PD-1–PD-L1 blockade fundamentally altered the way that diabetogenic T cells interacted with antigen-bearing $CD11c^+$ DCs.

PD-L1 blockade promotes T cell activation

Anergy induced in BDC2.5 T cells exposed to the p31-pulsed, fixed APCs led to a defect in early TCR signaling events, including Ca^{2+} flux (**Fig. 1**) and Erk phosphorylation[10,36]. However, treatment of anergic T cells with phorbol 12-myristate 13-acetate and ionophore reversed tolerance and promoted T cell activation (**Fig. 1** and data not shown). Thus, any therapy that would break tolerance in this system would be expected to reverse this TCR signaling defect. To correlate our single-cell imaging data with functional measures of T cell activation, we assayed Erk phosphorylation in p31-SP-tolerized BDC2.5 TCR–transgenic T cells by flow cytometry. We collected antigen-specific, tolerized BDC2.5 T cells 5 h after *in vivo* injection of anti-PD-L1 or isotype-matched control antibody and stained the cells with phosphorylation-specific antibodies both immediately and after stimulation with phorbol 12-myristate 13-acetate (**Fig. 5e**). Tolerized T cells did not show Erk phosphorylation after *in vivo* APC engagement[36–38] (**Fig. 5e**). In contrast, treatment with anti-PD-L1 resulted in substantial Erk phosphorylation in tolerized T cells, but treatment with isotype-matched control antibody did not (**Fig. 5f**). These results indicate that proximal TCR signaling components, including Erk phosphorylation, are restored after PD-1–PD-L1 blockade.

Effective TCR signaling culminates in the production of effector cytokines. Tolerence induced by p31-SP resulted in lower amounts of inflammatory cytokines, including IL-2 and interferon (IFN-γ), in the PLNs[10]. Here we bred antigen-specific NOD BDC2.5 TCR–transgenic mice with 'Yeti' mice, which express a YFP reporter cassette under the control of the promoter of the gene encoding IFN-γ[31]. We transferred tolerized BDC2.5 Thy-1.1^+ Yeti T cells into recipient NOD mice and treated the recipient mice with isotype-matched control antibody, anti-PD-L1 or anti-CTLA-4. PD-L1 blockade abrogated tolerance, and most $CD4^+$ T cells isolated directly from the islets of mice injected with anti-PD-L1 produced IFN-γ (57.8% ± 5.5%; **Fig. 5g**). These results demonstrate a T cell–intrinsic abrogation of anergy, and we did not detect this effect when we administered anti-CTLA-4 or isotype-matched control antibody (6.3% ± 1.8% or 5.5% ± 1.3%, respectively ($P < 0.0001$); **Fig. 5g**). Together these findings indicate that PD-L1 blockade restored the ability of anergic T cells to engage in prolonged DC interactions, produce inflammatory cytokines and induce rapid development of type 1 diabetes.

DISCUSSION

In this study, we sought to determine the roles of the inhibitory receptors PD-1 and CTLA-4 on T cell migration during the maintenance of tolerance. Our results have indicated that disruption of PD-1–PD-L1 interactions enhanced the interactions of tolerized T cells with antigen-bearing DCs and facilitated the phosphorylation of key TCR signaling molecules, but disruption of CTLA-4–B7 interactions did not. This T cell engagement with antigen-bearing DCs ultimately resulted in the production of effector cytokines and rapid progression of autoimmunity.

The duration of T cell–DC contacts and its influence on T cell activation and the induction of tolerance has been a topic of great interest. Several published reports have shown that during the induction of T cell tolerance, both transient and stable DC interactions can occur[20,23]. During the process of T cell activation, the duration of T cell–DC contacts is highly variable *in vivo*, ranging from minutes to several hours[39]. Early reports suggested that initial interactions during the first phase of T cell activation tend to be transient (5–10 min during the first 3–15 h)[20,21,40]. However, a subsequent report found that long lived T cell–DC interactions can occur after the initial T cell–DC contact and that prolonged interactions are required for T cell activation[41]. In this study, Erk phosphorylation occurred early after stable T cell–DC conjugates were formed, and IFN-γ production increased with longer T cell–DC interactions[41]. These interactions required TCR engagement of complexes of peptide and major histocompatibility complex class II, as blockade of major histocompatibility complex class II *in vivo* terminated stable contacts, resulted in greater T cell motility, led to less T cell proliferation, and prevented IFN-γ production. The second phase of T cell activation subsequently results in contacts of longer duration, in which T cells form stable conjugates and begin to secrete cytokines. During phase three, T cell motility increases and cell proliferation occurs[21]. Our studies have demonstrated that PD-1 blockade restored stable T cell–DC contacts, Erk phosphorylation, IFN-γ production and, most notably, type 1 diabetes. These findings suggest that PD-1 normally functions to prevent the T cell stop signal and the formation of stable conjugates with antigen-bearing DCs.

Anergic T cells have been shown *in vitro* to form unstable immunological synapses with allogeneic APCs and to fail to recruit the signaling proteins necessary to initiate T cell activation[42]. We suggest that these transient interactions are required in our system (but are impossible to discern *in vivo*), as the breakdown of tolerance after PD-1–PD-L1 blockade only occurred when antigen was

present, as in PLNs and pancreas, and did not occur in the ILNs. Thus, abrogation of tolerance allows the stabilization of these interactions, which permits full T cell activation and clinical disease.

Reports suggest that B7-1 and PD-L1 interact directly with each other to negatively regulate T cells[13]. Thus far, however, *in vivo* data to support the functionality of this interaction have not been reported. Our data do not suggest that this interaction was responsible for the tolerant phenotype in the present study, as administration of anti-B7-1 had no effect on T cell velocity, track displacement or movement trajectories relative to the effects produced by isotype-matched control antibody (data not shown). In addition, PD-1-blocking antibodies had effects similar to those of PD-L1 (data not shown). Finally, tolerized BDC2.5 T cells arrested and stopped when transferred into PD-L1-deficient (*Cd274*$^{-/-}$) recipients, similar to the movement in experiments with PD-L1 antibody blockade (data not shown), which supports the idea that PD-1–PD-L1 interactions are critical for tolerance.

Blockade of CTLA-4–B7 interactions can prevent the induction of tolerance by peptide-pulsed fixed APCs but cannot reverse tolerance once it is established[10]. We detected no influence of CTLA-4 on the migratory activity of tolerized T cells in these conditions. It is notable that we used the same dose of blocking CTLA-4-specific antibody in our MPLSM experiments as was used in the previous study, which documented a critical role for CTLA-4 during the induction of tolerance[10]. Because of the complex nature of lattice formation with B7-1, we have also explored anti-CTLA-4 Fab fragments and obtained results similar to those obtained with intact anti-CTLA-4. The results presented here suggest that CTLA-4 inhibition has biological consequences that are different qualitatively and quantitatively from those of PD-1–PD-L1 blockade.

Although CTLA-4 and PD-1 both limit T cell signaling, cytokine production and cell cycle progression and may share potential targets, some key biochemical differences have been reported. After engagement of its ligand (PD-L1 or PD-L2), PD-1 can bind SHP-1 and SHP-2 (refs. 4,43). The binding of SHP-1 and SHP-2 can terminate early TCR signals by dephosphorylating key signaling intermediates, including the kinases Akt, PI(3)K, Zap70 and PKC-θ. Like PD-1, CTLA-4 can interact with SHP-1 and SHP-2 (ref. 14). Unlike PD-1, CTLA-4 can also interact with the phosphatase PP2a[15]. Another difference between these two inhibitory receptors is the structural motif used to bind phosphatases. CTLA-4 interacts through the immunoreceptor tyrosine-based inhibitory motif, whereas PD-1 contains an additional motif, the immunoreceptor tyrosine-based switch motif[43]. Mutation of sequence encoding the immunoreceptor tyrosine-based inhibitory motif has little effect on signaling, whereas mutations of sequence encoding the immunoreceptor tyrosine-based switch motif abrogate the ability of PD-1 to limit T cell population expansion[43]. This suggests that PD-1 and CTLA-4 use different structural motifs to bind and recruit phosphatases for signal blockade. Further work is needed to determine the precise biochemical relationship between these two potent negative regulatory molecules.

Genetic experiments may help to explain the different roles of PD-1 and CTLA-4 in immune homeostasis, breakdown of tolerance and establishment of autoimmunity. CTLA-4 deficiency results in rapid multiorgan tissue inflammation and death by 3–4 weeks of age, regardless of mouse genetic background[5], whereas autoimmunity in PD-1-deficient mice is slower and tissue specific in a manner dependent on genetic background[4]. Such reports suggest that deficiencies in the PD-1–PD-L1 pathway may potentiate tissue-specific autoimmune predispositions. The expression and distribution of CTLA-4 and PD-1 ligands may help explain these differences. The fundamental difference between the effects of CTLA-4 and PD-1 on T cell migration, as described here, may also help to explain these differences.

Two reports have investigated the effect of CTLA-4 on T cell stop signals[44,45]. One study found that CTLA-4$^+$ T cells fail to stop or slow down in response to *in vivo* peptide challenge and that anti-CTLA-4 increases T cell motility[44]. A follow-up study reported that CTLA-4-deficient T cells show considerable resistance to a stop signal induced by anti-CD3 (ref. 45). It is difficult to explain the discrepancies between those studies, but they may be due to subtle differences between sorted T cell subpopulations, CTLA-4 surface stability, blocking antibodies or use of knockout T cells. Here we found no influence of CTLA-4 blockade on TCR-driven stop signals. In our study, CTLA-4 blockade did not alter the DC-binding properties of the tolerized T cells, did not result in substantial Erk phosphorylation, did not restore IFN-γ production and did not result in the rapid development of autoimmune diabetes. One major difference is that the previous reports tracked the migration of naive T cells during primary stimulation[44,45], whereas our studies here focused on anergic T cells during the reactivation phase.

Finally, it is notable that PD-1–PD-L1 blockade resulted in greater accumulation and/or enhanced proliferation of antigen-specific T cells in the target tissue[10]. This finding supports the idea that T cell–DC interactions serve a key role during tissue-specific reactivation. Future work in this area should determine if CD4$^+$ T cells interact directly with islet target cells or through a tissue-specific major histocompatibility complex class II–positive cell. Further investigation of the signals that maintain tolerance in this and similar settings will aid in the understanding of how to exploit the PD-1–PD-L1 pathway in efforts to prevent and treat autoimmunity, promote transplant acceptance and limit tumor growth.

METHODS

Methods and any associated references are available in the online version of the paper at http://www.nature.com/natureimmunology/.

Note: Supplementary information is available on the Nature Immunology website.

ACKNOWLEDGMENTS

We thank M. Hara and G. Bell (University of Chicago) for C57BL/6 MIP.eGFP mice; M. Nussenzweig (Rockefeller University) for C57BL/6 CD11c-YFP mice; A. Sharpe (Harvard Medical School) for C57BL/6 PD-L1-deficient mice; C. Benoist and D. Mathis (Harvard Medical School) for NOD BDC2.5 TCR–transgenic mice; R. Locksley (University of California, San Francisco) for Yeti (IFN-γ reporter) mice; N. Martenier for animal care; C. Allen, E. Finger, E. Peterson, R. Freidman, K. Hogquist, C. Penaranda and X. Zhou for scientific discussions; G. Szot and P. Koudria for islet transplantation; C. McArthur for cell sorting; and A. Bullen and M. Jenkins for multiphoton imaging support. Supported by LifeScan, the US National Institutes of Health (AI35297 to J.A.B., and P30 DK63720 for core support), the Juvenile Diabetes Research Foundation (10-2006-799 to B.T.F.), the American Diabetes Association (7-09-JF-21 to B.T.F.) and the University of Minnesota Medical School (B.T.F.).

AUTHOR CONTRIBUTIONS

B.T.F. and J.A.B. designed and conceptualized the research project; B.T.F., K.E.P, T.O. and J.W. did the experiments; B.T.F., T.N.E., Q.T. and M.F.K. analyzed the data; B.T.F prepared the figures; B.T.F. and J.A.B. interpreted the data and wrote the manuscript; and M.A. provided anti-PD-L1 hybridoma.

Published online at http://www.nature.com/natureimmunology/.
Reprints and permissions information is available online at http://npg.nature.com/reprintsandpermissions/.

1. Walunas, T.L. *et al.* CTLA-4 can function as a negative regulator of T cell activation. *Immunity* **1**, 405–413 (1994).

2. Luhder, F., Chambers, C., Allison, J.P., Benoist, C. & Mathis, D. Pinpointing when T cell costimulatory receptor CTLA-4 must be engaged to dampen diabetogenic T cells. *Proc. Natl. Acad. Sci. USA* **97**, 12204–12209 (2000).
3. Chikuma, S., Imboden, J.B. & Bluestone, J.A. Negative regulation of T cell receptor-lipid raft interaction by cytotoxic T lymphocyte-associated antigen 4. *J. Exp. Med.* **197**, 129–135 (2003).
4. Keir, M.E., Butte, M.J., Freeman, G.J. & Sharpe, A.H. PD-1 and its ligands in tolerance and immunity. *Annu. Rev. Immunol.* **26**, 677–704 (2008).
5. Tivol, E.A. *et al.* Loss of CTLA-4 leads to massive lymphoproliferation and fatal multiorgan tissue destruction, revealing a critical negative regulatory role of CTLA-4. *Immunity* **3**, 541–547 (1995).
6. Nishimura, H., Minato, N., Nakano, T. & Honjo, T. Immunological studies on PD-1 deficient mice: implication of PD-1 as a negative regulator for B cell responses. *Int. Immunol.* **10**, 1563–1572 (1998).
7. Yamazaki, T. *et al.* Expression of programmed death 1 ligands by murine T cells and APC. *J. Immunol.* **169**, 5538–5545 (2002).
8. Ishida, M. *et al.* Differential expression of PD-L1 and PD-L2, ligands for an inhibitory receptor PD-1, in the cells of lymphohematopoietic tissues. *Immunol. Lett.* **84**, 57–62 (2002).
9. Barber, D.L. *et al.* Restoring function in exhausted CD8 T cells during chronic viral infection. *Nature* **439**, 682–687 (2006).
10. Fife, B.T. *et al.* Insulin-induced remission in new-onset NOD mice is maintained by the PD-1-PD-L1 pathway. *J. Exp. Med.* **203**, 2737–2747 (2006).
11. Keir, M.E. *et al.* Tissue expression of PD-L1 mediates peripheral T cell tolerance. *J. Exp. Med.* **203**, 883–895 (2006).
12. Ansari, M.J. *et al.* The programmed death-1 (PD-1) pathway regulates autoimmune diabetes in nonobese diabetic (NOD) mice. *J. Exp. Med.* **198**, 63–69 (2003).
13. Butte, M.J., Keir, M.E., Phamduy, T.B., Sharpe, A.H. & Freeman, G.J. Programmed death-1 ligand 1 interacts specifically with the B7–1 costimulatory molecule to inhibit T cell responses. *Immunity* **27**, 111–122 (2007).
14. Chikuma, S. & Bluestone, J.A. CTLA-4 and tolerance: the biochemical point of view. *Immunol. Res.* **28**, 241–253 (2003).
15. Parry, R.V. *et al.* CTLA-4 and PD-1 receptors inhibit T-cell activation by distinct mechanisms. *Mol. Cell. Biol.* **25**, 9543–9553 (2005).
16. Schneider, H. & Rudd, C.E. Tyrosine phosphatase SHP-2 binding to CTLA-4: absence of direct YVKM/YFIP motif recognition. *Biochem. Biophys. Res. Commun.* **269**, 279–283 (2000).
17. Fife, B.T. & Bluestone, J.A. Control of peripheral T-cell tolerance and autoimmunity via the CTLA-4 and PD-1 pathways. *Immunol. Rev.* **224**, 166–182 (2008).
18. Germain, R.N., Miller, M.J., Dustin, M.L. & Nussenzweig, M.C. Dynamic imaging of the immune system: progress, pitfalls and promise. *Nat. Rev. Immunol.* **6**, 497–507 (2006).
19. Bousso, P. & Robey, E.A. Dynamic behavior of T cells and thymocytes in lymphoid organs as revealed by two-photon microscopy. *Immunity* **21**, 349–355 (2004).
20. Hugues, S. *et al.* Distinct T cell dynamics in lymph nodes during the induction of tolerance and immunity. *Nat. Immunol.* **5**, 1235–1242 (2004).
21. Mempel, T.R., Henrickson, S.E. & Von Andrian, U.H. T-cell priming by dendritic cells in lymph nodes occurs in three distinct phases. *Nature* **427**, 154–159 (2004).
22. Miller, M.J., Wei, S.H., Parker, I. & Cahalan, M.D. Two-photon imaging of lymphocyte motility and antigen response in intact lymph node. *Science* **296**, 1869–1873 (2002).
23. Shakhar, G. *et al.* Stable T cell-dendritic cell interactions precede the development of both tolerance and immunity in vivo. *Nat. Immunol.* **6**, 707–714 (2005).
24. Bajenoff, M. *et al.* Stromal cell networks regulate lymphocyte entry, migration, and territoriality in lymph nodes. *Immunity* **25**, 989–1001 (2006).
25. Negulescu, P.A., Krasieva, T.B., Khan, A., Kerschbaum, H.H. & Cahalan, M.D. Polarity of T cell shape, motility, and sensitivity to antigen. *Immunity* **4**, 421–430 (1996).
26. Dustin, M.L., Bromley, S.K., Kan, Z., Peterson, D.A. & Unanue, E.R. Antigen receptor engagement delivers a stop signal to migrating T lymphocytes. *Proc. Natl. Acad. Sci. USA* **94**, 3909–3913 (1997).
27. Hurez, V. *et al.* Restricted clonal expression of IL-2 by naive T cells reflects differential dynamic interactions with dendritic cells. *J. Exp. Med.* **198**, 123–132 (2003).
28. Benvenuti, F. *et al.* Dendritic cell maturation controls adhesion, synapse formation, and the duration of the interactions with naive T lymphocytes. *J. Immunol.* **172**, 292–301 (2004).
29. Scholer, A., Hugues, S., Boissonnas, A., Fetler, L. & Amigorena, S. Intercellular adhesion molecule-1-dependent stable interactions between T cells and dendritic cells determine CD8$^+$ T cell memory. *Immunity* **28**, 258–270 (2008).
30. Judkowski, V. *et al.* Identification of MHC class II-restricted peptide ligands, including a glutamic acid decarboxylase 65 sequence, that stimulate diabetogenic T cells from transgenic BDC2.5 nonobese diabetic mice. *J. Immunol.* **166**, 908–917 (2001).
31. Tang, Q. *et al.* Visualizing regulatory T cell control of autoimmune responses in nonobese diabetic mice. *Nat. Immunol.* **7**, 83–92 (2006).
32. Lindquist, R.L. *et al.* Visualizing dendritic cell networks in vivo. *Nat. Immunol.* **5**, 1243–1250 (2004).
33. Sumen, C., Mempel, T.R., Mazo, I.B. & von Andrian, U.H. Intravital microscopy: visualizing immunity in context. *Immunity* **21**, 315–329 (2004).
34. Cahalan, M.D., Parker, I., Wei, S.H. & Miller, M.J. Two-photon tissue imaging: seeing the immune system in a fresh light. *Nat. Rev. Immunol.* **2**, 872–880 (2002).
35. Nishimura, H. *et al.* Developmentally regulated expression of the PD-1 protein on the surface of double-negative (CD4$^-$CD8$^-$) thymocytes. *Int. Immunol.* **8**, 773–780 (1996).
36. Macian, F. *et al.* Transcriptional mechanisms underlying lymphocyte tolerance. *Cell* **109**, 719–731 (2002).
37. Li, W., Whaley, C.D., Mondino, A. & Mueller, D.L. Blocked signal transduction to the ERK and JNK protein kinases in anergic CD4$^+$ T cells. *Science* **271**, 1272–1276 (1996).
38. Morton, A.M., McManus, B., Garside, P., Mowat, A.M. & Harnett, M.M. Inverse Rap1 and phospho-ERK expression discriminate the maintenance phase of tolerance and priming of antigen-specific CD4$^+$ T cells in vitro and in vivo. *J. Immunol.* **179**, 8026–8034 (2007).
39. Breart, B. & Bousso, P. Cellular orchestration of T cell priming in lymph nodes. *Curr. Opin. Immunol.* **18**, 483–490 (2006).
40. Miller, M.J., Safrina, O., Parker, I. & Cahalan, M.D. Imaging the single cell dynamics of CD4$^+$ T cell activation by dendritic cells in lymph nodes. *J. Exp. Med.* **200**, 847–856 (2004).
41. Celli, S., Lemaitre, F. & Bousso, P. Real-time manipulation of T cell-dendritic cell interactions in vivo reveals the importance of prolonged contacts for CD4$^+$ T cell activation. *Immunity* **27**, 625–634 (2007).
42. Zambricki, E. *et al.* In vivo anergized T cells form altered immunological synapses in vitro. *Am. J. Transplant.* **6**, 2572–2579 (2006).
43. Chemnitz, J.M., Parry, R.V., Nichols, K.E., June, C.H. & Riley, J.L. SHP-1 and SHP-2 associate with immunoreceptor tyrosine-based switch motif of programmed death 1 upon primary human T cell stimulation, but only receptor ligation prevents T cell activation. *J. Immunol.* **173**, 945–954 (2004).
44. Schneider, H. *et al.* Reversal of the TCR stop signal by CTLA-4. *Science* **313**, 1972–1975 (2006).
45. Downey, J., Smith, A., Schneider, H., Hogg, N. & Rudd, C.E. TCR/CD3 mediated stop-signal is decoupled in T-cells from Ctla4 deficient mice. *Immunol. Lett.* **115**, 70–72 (2008).

ONLINE METHODS

Mice. All mice were housed and bred in specific pathogen–free conditions in animal barrier facilities at the University of California, San Francisco or the University of Minnesota. C57BL/6 MIP.eGFP mice from M. Hara and G. Bell[46] were backcrossed for more than 12 generations to NOD mice. C57BL/6 CD11c-YFP mice from M. Nussenzweig[32] were backcrossed for more than ten generations to NOD mice. C57BL/6 PD-L1-deficient mice from A. Sharpe[11] were backcrossed for ten generations to NOD mice. Female NOD mice were from Taconic. NOD BDC2.5 TCR–transgenic mice from C. Benoist and D. Mathis[47] were crossed to NOD Thy-1.1$^+$ mice. Yeti (IFN-γ reporter) mice provided by R. Locksley were bred for ten generations to NOD mice and then were crossed with NOD Thy-1.1$^+$ BDC2.5 TCR–transgenic mice to generate NOD BDC2.5 Thy-1.1$^+$ Yeti mice[31]. NOD.SCID mice were from The Jackson Laboratory. Mice were 3–10-weeks-old at the initiation of the experiments. All animal experiments were approved by the Institutional Animal Care and Use Committee of the University of California, San Francisco and the University of Minnesota.

Antibodies. Fluorescein isothiocyanate–conjugated anti-CD4 (RM4-5), peridinin chlorophyll protein–conjugated anti-CD8a (Ly-2), allophycocyanin-conjugated anti-CD90.1 (HIS51) and phycoerythrin-conjugated anti-Vβ4 (KT4) were from BD Biosciences. Rabbit polyclonal antibody to Erk1 and Erk 2 (p44 and p42) phosphorylated at Thr202 and Tyr204 (9101L) was from Cell Signaling Technology[48]. Anti-PD-1 (RMP1-14), anti-PD-L1 (MIH5 and MIH6) and anti-PD-L2 (TY25) were made as described[7,10]. Hamster immunoglobulin G (007-000-003) and rat immunoglobulin G (012-000-003) were from Jackson ImmunoResearch Laboratories. Anti-CTLA-4 (UC4F10) and anti-CTLA-4 Fab fragments were made as described[1]. Mice were injected intraperitoneally with 250 μg isotype-matched control antibody, anti-PD-L1, anti-PD-L2, anti-B7-1, anti-PD-1 or anti-CTLA-4.

Antigens. Peptide p31 (YVRPLWVRME) was from Genemed Synthesis. The amino acid composition was verified by mass spectrometry, and purity (>98%) was assessed by high-performance liquid chromatography.

Cell culture, transfer and induction of tolerance. NOD Thy-1.1$^+$ BDC2.5.TCR–transgenic lymphocytes were collected and pooled from brachial, axillary, periaortic, pancreatic and inguinal lymph nodes and from the spleen. Cells were activated *in vitro* in the presence of 0.5 μM p31 peptide in complete DMEM containing 50 μM 2-mercaptoethanol, 2 mM L-glutamine, 100 U/ml of penicillin-streptomycin, 0.1 M nonessential amino acids (Invitrogen) and 10% (vol/vol) FCS (Hy-clone). Cells were incubated at 37 °C in a humidified atmosphere containing 5% CO_2. Cells were collected after 96 h and washed, and 5×10^6 T cells were transferred intravenously into naive prediabetic NOD recipients. Tolerance was induced by intravenous injection of 50×10^6 chemically treated antigen-coupled syngeneic splenocytes (p31 or sham control) as described[10].

Assessment of diabetes. Blood glucose concentrations in female NOD mice were measured with OneTouch glucose meters (LifeScan). Mice were considered diabetic with two consecutive readings of over 250 mg/dl.

Flow cytometry and cell sorting. For assessment of the expression of surface molecules and cytokines, cells were labeled with predetermined optimal antibody concentrations according to the manufacturer's staining protocol and 0.5×10^6 events in the CD4$^+$ gate were acquired as described[10]. Data were acquired on an LSR II and were analyzed with FACSDiva software (Becton Dickinson). NOD Thy-1.1$^+$ BDC2.5 lymph node cells and splenocytes were stained with fluorescein isothiocyanate–conjugated anti-CD4 and allophycocyanin-conjugated-anti-CD90.1 and were sorted with a MoFlo high-speed cell sorter (DakoCytomation). All sorted populations had a cell purity of 98% or more.

Isolation and transplantation of pancreatic islets. Islets were isolated as reported[49]. A solution of collagenase P (3 ml; 0.75 mg/ml; Roche) was injected into the pancreatic ducts of 4-week-old NOD MIP.eGFP mice. Distended pancreases were removed and were incubated for 17 min at 37 °C. Liberated free islets were purified by centrifugation on a Eurocollin-Ficoll gradient. Manually selected islets (400–500) were transplanted beneath the left renal capsule of each recipient[50].

MPLSM acquisition and analysis. A custom-built resonant-scanning instrument based on published designs containing four photomultiplier tubes operating at video rate was used for multiphoton microscopy[31]. For imaging of T cells, BDC2.5 CD4$^+$ CD90.1$^+$ T cells were sorted and labeled with Cell Tracker Orange CMTMR (5-(and-6)-(((4-chloromethyl) benzoyl) amino) tetramethyl rhodamine; Invitrogen) and were transferred into recipient mice. ILNs or PLNs were collected from recipients and immobilized on coverslips with the hilum facing away from the objective. Lymph nodes were maintained at 36 °C in RPMI medium bubbled with 95% O_2 and 5% CO_2 and were imaged through the capsule distal to the efferent lymphatic. Transplanted islets were imaged under the exposed kidney capsule maintained at 36 °C in RPMI medium bubbled with 95% O_2 and 5% CO_2. Samples were excited with a MaiTai TiSaphire laser (10 W; Spectra-Physics) tuned to a wavelength of 800–810 nm, and emission wavelengths of 500–540 nm (for carboxyfluorescein diacetate succinimidyl ester), 567–640 nm (for CMTMR) and 380–420 nm (for detection of second-harmonic emission) were collected. Each *xy* plane spanned 192 μm × 160 μm at a resolution of 0.4 μm per pixel and images of 44–46 *xy* planes with 2 μm *z* spacing were formed by averaging of 10–12 video frames every 30 s for 10–30 min. Images acquired were 70–250 μm below the lymph node capsule identified by the second-harmonic signal. Images were acquired with Video Savant software (IO Industries). Maximum-intensity *z*-projection time-lapse image sequences were generated with MetaMorph software (Molecular Devices). Three-dimensional rotations and time-lapse image sequences were generated with Imaris 5.7.2 x64 software (Bitplane). Semiautomated cell tracking in three dimensions was verified manually. Tracking data were analyzed in Microsoft Excel with a custom 'macro' program written in Microsoft Visual Basic for Applications. The motility coefficient $M = x^2 / 6t$ (where 'x' is the mean displacement and 't' is time) was calculated from the slope ($x / t^{1/2}$) obtained by regression analysis of the mean displacement (x) versus the square root of time ($t^{1/2}$) as described[33].

Statistical analysis. GraphPad Prism software was used for statistical comparisons of two groups; *P* values were calculated by the unpaired Student's *t*-test. For comparisons of multiple groups, *P* values were calculated by one-way analysis of variance with GraphPad Prism. *P* values of 0.05 or less were considered significant.

46. Hara, M. *et al.* Transgenic mice with green fluorescent protein-labeled pancreatic β-cells. *Am. J. Physiol. Endocrinol. Metab.* **284**, E177–E183 (2003).
47. Katz, J.D., Wang, B., Haskins, K., Benoist, C. & Mathis, D. Following a diabetogenic T cell from genesis through pathogenesis. *Cell* **74**, 1089–1100 (1993).
48. Hale, M.B. & Nolan, G.P. Phospho-specific flow cytometry: intersection of immunology and biochemistry at the single-cell level. *Curr. Opin. Mol. Ther.* **8**, 215–224 (2006).
49. Lenschow, D.J. *et al.* Inhibition of transplant rejection following treatment with anti-B7–2 and anti-B7–1 antibodies. *Transplantation* **60**, 1171–1178 (1995).
50. Szot, G.L., Koudria, P. & Bluestone, J.A. Transplantation of pancreatic islets into the kidney capsule of diabetic mice. *J. Vis. Exp.* **9**, 404 (2007).